Samireh Hosseini, Zahra Mardani*, Keyvan Moeini, Cameron Carpenter-Warren, Alexandra M.Z. Slawin and J. Derek Woollins

A binuclear Cd(II) complex containing bridging pyrimidine-based ligands

https://doi.org/10.1515/znb-2019-0193
Received October 14, 2019; accepted January 8, 2020

Abstract: In this work, a pyrimidine-based ligand, *N*′-(amino(pyrimidin-2-yl)methylene)pyrimidine-2-carbohydrazonamide hydrate ($APPH \cdot H_2O$), and its binuclear complex of cadmium, $[Cd(\mu\text{-}APPH)Br]_2$, **1**, were prepared and identified by elemental analysis, FT-IR, ^1H NMR spectroscopy as well as single-crystal X-ray diffraction. X-ray structure analysis of **1** revealed octahedrally coordinated cadmium centers with a CdN_4Br_2 environment containing two bridging APPH ligands; each APPH ligand acts as an N_4-donor (N_2-donor toward each cadmium atom) and forms two five-membered chelate rings that are approximately perpendicular to each other. In the network of **1**, the N–H···Br hydrogen bonds form motifs such as $R_2^2(12, 14)$, $R_6^6(24, 26, \ldots, 46)$. The crystal network is further stabilized by π-π stacking interactions between pyrimidine rings. The optimized structures of the ligand and complex were investigated along with their charge distribution patterns by density functional theory and natural bond orbital analysis, respectively.

Keywords: bromide; binuclear; cadmium(II) complex; DFT; pyrimidine.

1 Introduction

Pyrimidines are a group of six-membered aromatic heterocycles [1] that are important chemical compounds due to their wide application in the pharmaceutical field [2–5]. The ability of the pyrimidine ring nitrogen atoms to act as a chelating ligand enables such compounds to be used to form supramolecular assemblies and as sensors [6]. For example, they have applications in light sensors for color-sensitive solar cells [7] and polarity sensors [8]. They are used for a diverse range of applications [9, 10].

To extend the chemistry of this class of compounds, in this work, the preparation, characterization (elemental analysis, FT-IR, ^1H NMR spectroscopy), and crystal structure of a new cadmium(II) complex, $[Cd(\mu\text{-}APPH)Br]_2$ (**1**), with *N*′-(amino(pyrimidin-2-yl)methylene)pyrimidine-2-carbohydrazonamide (APPH) as a ligand (Scheme 1) is presented. The structure of the isolated molecules of $APPH^{opt}$ and $\mathbf{1}^{opt}$ have been determined by density functional theory (DFT) studies to compare the results with the solid-state data. The variation of the charge values of atoms/ions during the complexation process was investigated by natural bond orbital (NBO) analysis.

2 Results and discussion

The $APPH \cdot H_2O$ ligand was prepared by the condensation of pyrimidine-2-carbonitrile and hydrazine hydrate. Reaction between cadmium(II) bromide and $APPH \cdot H_2O$ provided complex **1**. The complex is air-stable and soluble in DMSO.

2.1 Spectroscopic studies

In the IR spectrum of the APPH, there are two bands in the range of 3250–3350 cm^{-1}, due to the primary amine group. These bands are shifted by 25 and 11 cm^{-1} to lower frequencies after coordination of the ligand to the cadmium atom. Although the crystallographic data shows that there is no bond between the amine functionality and the cadmium atom, these shifts can be attributed to the changes in electron density of this group after coordination to the cadmium atom and to H bonding. The ν (C=N) vibrations arising from imine and pyrimidine units of the ligand are observed at approximately 1600 cm^{-1} with only

***Corresponding author: Zahra Mardani,** Inorganic Chemistry Department, Faculty of Chemistry, Urmia University, 57561-51818 Urmia, Islamic Republic of Iran, e-mail: z.mardani@urmia.ac.ir
Samireh Hosseini: Inorganic Chemistry Department, Faculty of Chemistry, Urmia University, 57561-51818 Urmia, Islamic Republic of Iran
Keyvan Moeini: Chemistry Department, Payame Noor University, 19395-4697 Tehran, Islamic Republic of Iran
Cameron Carpenter-Warren and Alexandra M.Z. Slawin: EaStCHEM School of Chemistry, University of St Andrews, St Andrews, Fife KY16 9ST, United Kingdom
J. Derek Woollins: EaStCHEM School of Chemistry, University of St Andrews, St Andrews, Fife KY16 9ST, United Kingdom; and Khalifa University, P.O. Box 127788, Abu Dhabi, United Arab Emirates

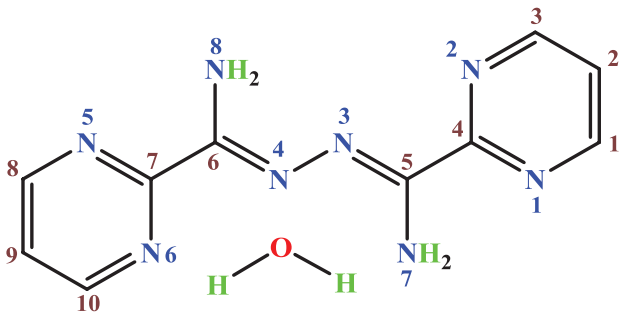

Scheme 1: Structure of the APPH · H_2O with atom labeling.

minor shifts. The presence of the water molecule in **1** gives rise to broad peaks in the ranges of 3300–3400 cm^{-1} and 1624 cm^{-1} [11, 12].

The ^1H NMR spectrum of the ligand confirms that the structure contains aromatic ($\delta = 7.59–8.93$ ppm) and aliphatic ($\delta = 5.19$ ppm) portions. The two hydrogen atoms nearest to the nitrogen atoms of the pyrimidine ring are observed as a doublet and another one in the *para* position as a triplet. The amine protons are observed as a broad singlet peak near $\delta = 6.6$ ppm.

2.2 Crystal and molecular structure of [Cd(μ-APPH)Br]$_2$ (1)

X-ray analysis of **1** (Fig. 1) reveals a binuclear structure with bridging APPH ligands. Each cadmium atom is coordinated by two N_2-donor APPH (each APPH totally acts as an N_4-donor) and two bromo ligands in a distorted octahedral arrangement (Figs. 1 and 2). The ligands have *cis* orientation. Study of the CSD database [13] reveals that there is one iron complex containing the APPH ligand [14], but the authors used a 1,2,4,5-tetrazine derivative as a starting ligand and then the APPH ligand was formed during the complexation process by a tetrazine-ring opening reaction. There are seven examples for a $Cd(NN)_2(Br^{terminal})_2$ (NN: each N_2-donor ligand forms a five-membered chelate ring) environment [11, 12, 15–19]. In these structures similar to **1**, the two bromo ligands have *cis* geometry except for one case [18]. The Cd–Br bond lengths average for *cis* isomers (2.645 Å) is 0.255 Å (0.253 Å for **1**) smaller than for the *trans* isomer (2.900 Å).

In **1**, each APPH ligand acts as a tetradentate $N_2^{imine}N_2^{pyrimidine}$-donor toward two cadmium atoms and forms an almost planar five-membered chelate ring (maximum deviation from a mean plane through the chelate ring: 0.087 Å for C5 and C7 atoms) around each cadmium atom. A six-membered 2L:2M^{1,4} ring (1 and 4 refer to the positions of the cadmium atoms in the ring) forms by participation of two APPH and two cadmium atoms [20].

In the crystal network of **1**, there are weak C–H···N, C–H···Br, and N–H···Br hydrogen bonds. Among them, the N–H···Br hydrogen bonds participate in the formation of a variety of different motifs [21, 22] such as $R_2^2(12)$, $R_2^2(14)$, $R_6^6(24)$, $R_6^6(26)$, $R_6^6(28)$, $R_6^6(30)$, $R_6^6(32)$, $R_6^6(34)$, $R_6^6(36)$, $R_6^6(38)$, $R_6^6(40)$, $R_6^6(42)$, $R_6^6(44)$, $R_6^6(46)$ (Fig. 2). In addition to these hydrogen bonds, the packing

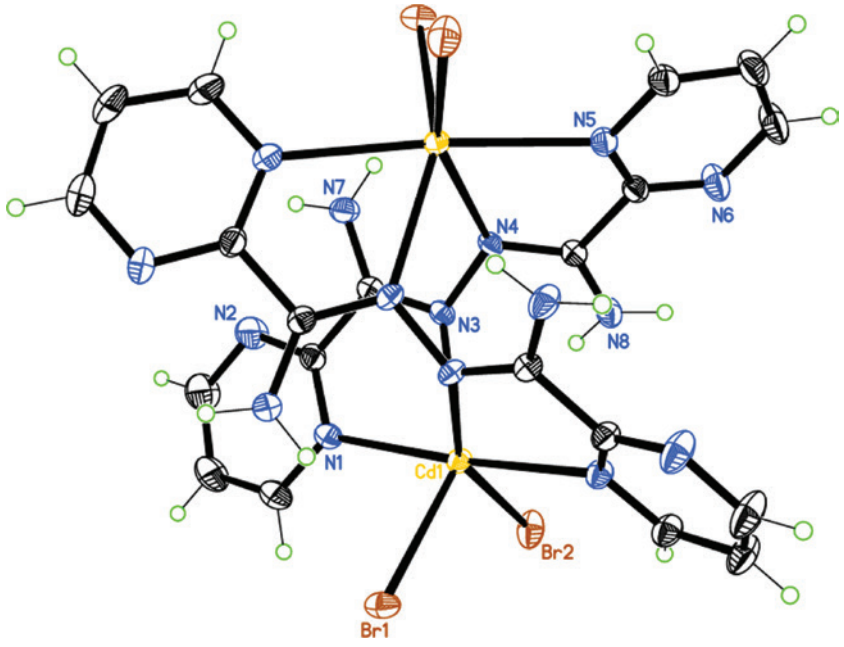

Fig. 1: ORTEP-III diagram of the molecular structure of complex **1**. The ellipsoids are drawn at the 50% probability level.

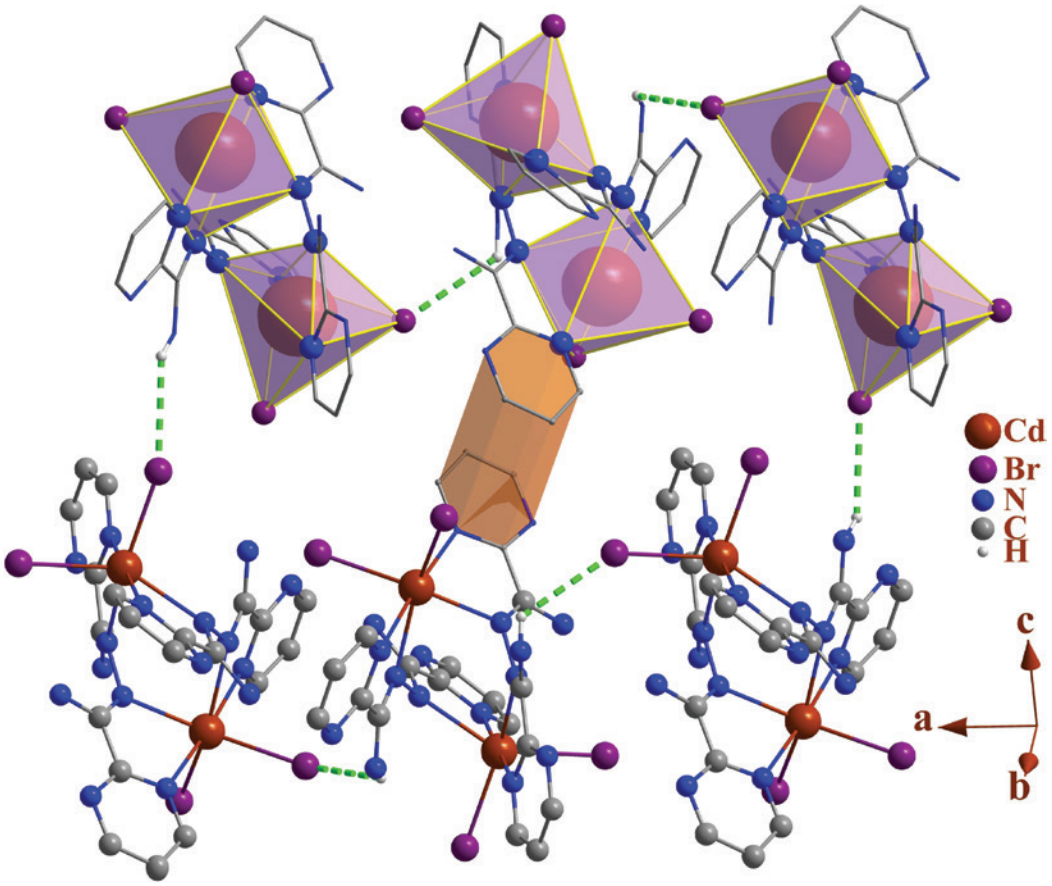

Fig. 2: Packing of molecules **1** in the crystal showing the $R_6^6(46)$ hydrogen bond motifs. Each CdN_4Br_2 unit is shown as an octahedron (lavender highlights). π-π stacking interaction is highlighted as orange.

features π-π stacking interactions [23, 24] between pyrimidine rings (Fig. 2). In this pattern, the rings are not exactly on top of each other and two rings have an anti-direction (centroid–centroid distance: 3.983 Å, angle between planes: 0°, perpendicular distance: 3.564 Å, slippage: 1.778 Å).

2.3 Theoretical studies

To enable a comparison of the geometrical parameters of complex **1** with its optimized analogue (**1**^{opt}, Fig. 3a), DFT calculations were performed for one isolated molecule. Among the different bond lengths of **1**^{opt}, two Cd–Br and one Cd–N3 bonds are approximately 0.1 Å longer than the corresponding bonds in **1** whereas others are comparable. The dihedral angle between mean planes through two five-membered chelate rings with *cis* position in **1**^{opt} and **1** is 56.10° and 60.64(4)°, respectively, indicating that the octahedral geometry of the cadmium atom in the solid phase is more perfect than the isolated form and The Br–Cd–Br angles in **1**^{opt} and **1** are 115.78° and 102.275(7)°, respectively.

Optimization of the APPH ligand reveals a *Z*/*Z* isomer (Fig. 3b) in which two amine groups have an *anti*-position (similar to Scheme 1). Maximum deviations of the atoms from a mean plane through the nonhydrogen atoms of the APPH molecule were observed for N^7 (0.205 Å) and C^2 (0.105 Å), which means that the ligand is almost planar and the amine groups are bent slightly from the molecule plane. Comparing this structure with that of **1** and **1**^{opt} reveals that the deviation from planarity of the ligand after complexation to the cadmium atom is increased. In **1** and **1**^{opt}, the dihedral angle between the mean planes through the two heterocycles is 67.32(4)° and 68.52°, respectively for **1** and **1**^{opt}.

To study the charge distribution before and after complexation, an NBO analysis was done on the free ligand (without the water molecule) and on **1**^{opt} (Table 1). Based on the calculated charge average for N atoms, the charges on the coordinated nitrogen atoms (N^a and N^c, Scheme 1) become more negative after coordination. Also, as is typical, the charge on the cadmium atom (+1.14) is lower

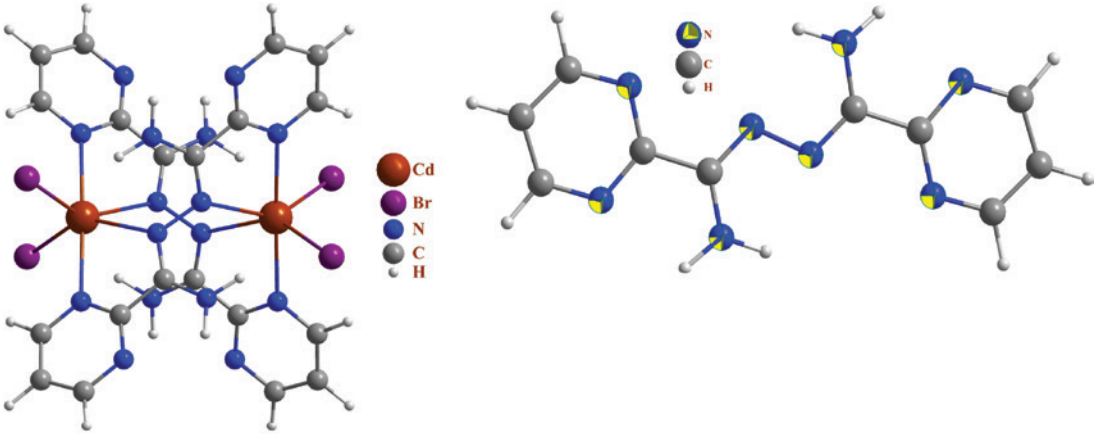

Fig. 3: Optimized structure of the complex $\mathbf{1}^{opt}$ (a) and APPH ligand (b).

Table 1: The NBO analysis results for $APPH^{opt}$ and $\mathbf{1}^{opt}$. Values are the average of charge on similar atoms.

	$C^{2,9}$	$C^{1,3,8,10}$	$C^{4,7}$	$C^{5,6}$	$H(C^a)$	$H(C^b)$	$H(N^b)$	$N^{1,2,5,6}$	$N^{7,8}$	$N^{3,4}$	Br	Cd
$APPH^{opt}$	−0.32	0.05	0.39	0.39	0.25	0.23	0.44	−0.47	−0.84	−0.38	–	–
$\mathbf{1}^{opt}$	−0.27	0.12	0.44	0.46	0.24	0.24	0.44	−0.55	−0.81	−0.47	−0.67	1.14

than the formal charge (+2) owing to electron donation of the ligands upon complexation [25, 26].

3 Conclusion

In this work, a new binuclear complex of cadmium(II), $[Cd(\mu\text{-APPH})Br]_2$ (**1**); APPH: *N′*-(amino(pyrimidin-2-yl) methylene)pyrimidine-2-carbohydrazonamide, and the hydrate of this pyrimidine-based ligand, $APPH \cdot H_2O$, were synthesized and their spectral properties were investigated. The crystal structure of the complex has been determined, in which the cadmium atom has a CdN_4Br_2 environment with a distorted octahedral geometry formed by two *cis*-N_2-donor APPH ligands (each ligand acts as N_4-donor toward two cadmium atoms) and two *cis*-bromo ligands. Two APPH ligands bridge two cadmium atoms to form a six-membered $2L{:}2M^{1,4}$ ring. In the crystals of **1**, the N–H···Br interactions form different types of hydrogen bonding motifs including, $R_2^2(12, 14)$, $R_6^6(24, 26, \ldots, 46)$, and there are π-π stacking interactions between pyrimidine rings on adjacent ligands. DFT calculations reveal that the octahedral geometry of the cadmium atom observed in the solid phase is closer to ideal than in the isolated molecule. An NBO analysis of both the nitrogen and carbon atoms was carried out to follow the effect of the donor/acceptor interaction.

4 Experimental

4.1 Materials and measurements

All starting chemicals and solvents were reagent or analytical grade and used as received. The infrared spectra of KBr pellets in the range of 4000–400 cm^{-1} were recorded with a FT-IR TENSOR 27 spectrometer. ^1H NMR spectrum was recorded on a Bruker Aspect 3000 instrument. The carbon, hydrogen, and nitrogen contents were determined by a Thermo Finnigan Flash Elemental Analyzer 1112 EA. The melting point was determined with a Barnsted Electrothermal 9200 electrically heated apparatus.

4.2 Preparation of *N′*-(amino(pyrimidin-2-yl)methylene)pyrimidine-2-carbohydrazonamide hydrate, $APPH \cdot H_2O$

The APPH ligand was prepared as described in the literature [27] with modifications. The spectral data of this ligand have not been reported previously and are presented in this work. A total of 1.91 g (38.15 mmol) of hydrazine hydrate, dissolved in methanol (10 mL), was added

dropwise with stirring to 2.00 g (19.03 mmol) of pyrimidine-2-carbonitrile in methanol (10 mL) under reflux for 10 h. The resultant precipitate was filtered off (yield: 0.62 g, 25%). A small amount of the ligand was formed from the filtrate solution; after solvent evaporation at room temperature, an oily compound was formed. After the addition of 5 mL of acetone to this compound and immersing it in an ultrasonic bath for 5 min, the precipitate was separated from the oil and collected by filtration (yield: 0.29 g, 12%). M. p. 187°C. – Anal. calcd. for $C_{10}H_{12}N_8O$ (260.26): C 46.15, H 4.65, N 43.06; found C 46.25, H 4.66, N 43.28%. – IR (KBr disk): ν_{as} = 3427 (H_2O), ν_s = 3358 (H_2O) and/or ν_{as} (NH_2), ν_s = 3276 (NH_2), ν = 3068 (C–H)^{ar}, ν = 1624 (C=N)^{imine} and/or δ (H_2O) and/or δ (NH_2), 1559 (C=N)^{pyrimidine}, ν = 1199 (C–N), ν = 1092 (N–N), ρ_r = 632 (H_2O), ρ_w = 545 (H_2O) cm^{-1}. –^{1}H NMR (300 MHz, DMSO-d_6): δ = 8.93) d, 4H, C^{1}H, C^{3}H, C^{8}H, C^{10}H, J = 4.8 Hz), 7.59) t, 2H, C^{2}H, C^{9}H, J = 4.8 Hz), 6.61 (s, 4H, NH_2) ppm.

4.3 Preparation of [Cd(μ-APPH)Br]$_2$

$CdBr_2$ (1.92 mmol, 0.52 g) was dissolved in methanol (10 mL) and added with stirring to the methanol solution (10 mL) of APPH · H_2O (1.92 mmol, 0.50 g). The reaction mixture was refluxed for 5 h. The solution was left to slowly evaporate at room temperature. The resulting yellow precipitate was filtered off and recrystallized from DMF. Yield 0.80 g, 81%. M. p. 234°C. – Anal. calcd. for $C_{10}H_{10}Br_2CdN_8$ (514.48): C 23.35, H 1.96, N 21.78; found C 23.39, H 2.03, N 21.91%. – IR (KBr disk): ν_{as} = 3333 (NH_2), ν_s = 3265 (NH_2), ν = 3060 (C–H)^{ar}, ν = 1632 (C=N)^{imine} and/or δ (NH_2), 1567 (C=N)^{pyrimidine}, ν = 1208 (C–N), ν = 1063 (N–N) cm^{-1}.

4.4 Crystal structure determination

X-ray diffraction data for **1** was collected at T = 93 K using a Rigaku FR-X Ultrahigh Brilliance Microfocus RA generator/confocal optics with an XtaLAB P200 diffractometer. MoKα radiation (λ = 0.71073 Å) was used and intensity data was collected using ω steps accumulating area detector images spanning at least a hemisphere of reciprocal space. All data was corrected for Lorentz polarization effects. A multiscan absorption correction was applied by using CrysAlis Pro [28]. The structure was solved using the intrinsic phasing method (Shelxt [29]) and refined by full-matrix least-squares against F^2 (Shelxl-2013 [30]). Nonhydrogen atoms were refined anisotropically, and the amine hydrogens were refined freely from the electron density map with some light geometrical restraints whereas all other hydrogen atoms were refined geometrically using a riding model. All calculations were performed using Olex 2 [31]. Diagrams of the molecular structure were created using Ortep-III [32, 33] and Diamond [34]. Selected crystallographic data is presented in Table 2. Selected bond lengths are displayed in Table 3 and hydrogen bond geometries in Table 4.

CCDC 1958990 contains the supplementary crystallographic data for this article. These data can be obtained free of charge from The Cambridge Crystallographic Data Centre via www.ccdc.cam.ac.uk/data_request/cif.

Table 2: Crystal structure data and structure refinement of complex **1**.

Empirical formula	$C_{20}H_{20}Br_4Cd_2N_{16}$
Formula weight, g mol^{-1}	1028.96
Crystal size, mm^3	0.24 × 0.06 × 0.06
Temperature, K	93
Crystal system	Monoclinic
Space group	*I*2/*a*
Unit cell dimensions	
a, Å	14.8169(2)
b, Å	11.8677(1)
c, Å	18.7709(2)
β, deg	105.472(1)
Volume, Å^3	3181.11(6)
Z	4
Calculated density, g cm^{-3}	2.15
Absorption coefficient, mm^{-1}	6.4
F(000), *e*	1952
θ range data collection, deg	2.2–28.4
h, *k*, *l* ranges	$-19 \le h \le 19$, $-14 \le k \le 15$, $-24 \le l \le 23$
Reflections collected/ independent/R_{int}	45,474/3666/0.022
Data/ref. parameters	3666/206
*R*1/*wR*2 ($I > 3\,\sigma(I)$)	0.0145/0.0396
*R*1/*wR*2 (all data)	0.0152/0.0398
Goodness-of-fit on F^2	1.09
Largest diff. peak/hole, *e* Å^{-3}	0.52/–0.20

Table 3: Selected bond lengths (Å) and angles (deg) for complex **1** with estimated standard deviations in parentheses.[a]

Bond lengths	1	1^{opt}	Angles	1
Cd1–Br1	2.6611(2)	2.768	Br2–Cd1–Br1	102.275(7)
Cd1–Br2	2.6329(2)	2.768	N1–Cd1–Br1	89.98(3)
Cd1–N1	2.4492(15)	2.483	N1–Cd1–Br2	91.61(3)
Cd1–N3	2.3841(13)	2.444	N1–Cd1–N4^i	108.85(5)
Cd1–N4^i	2.4527(13)	2.484	N3–Cd1–Br1	145.56(3)
Cd1–N5^i	2.4353(14)	2.444	N3–Cd1–Br2	104.17(3)

[a]Symmetry operator: ^{i} $-x+1/2, y, -z+1$.

Table 4: Hydrogen bond dimensions (Å and deg) in complex **1**.[a]

D–H···A	*d*(D–H)	*d*(H···A)	*d*(D···A)	<(DHA)	Symmetry code of atoms A
C3–H3···Br2	0.930	2.8153	3.640(2)	148.4	0.5–*x*, 1.5–*y*, 1.5–*z*
C2–H2···Br1	0.930	2.7643	3.686(2)	171.3	1–*x*, 0.5+*y*, 1.5–*z*
C10–H10···N6	0.930	2.670	3.526(3)	153.2	–*x*, –*y*, 1–*z*
C9–H9···Br1	0.930	2.9123	3.617(2)	133.6	–0.5+*x*, –0.5+*y*, –0.5+*z*
N8–H8a···Br1	0.87	2.93	3.523(2)	127	–0.5+*x*, 1–*y*, *z*
N8–H8b···Br2	0.88	2.84	3.452(2)	127	0.5–*x*, 0.5–*y*, 1.5–*z*

4.5 Computational details

The structures were optimized using GAUSSIAN 09 software [35] and calculated for an isolated molecule using DFT [36] at the B3LYP/6-31G(d,p) [37, 38] level of theory for the ligand and B3LYP/LanL2DZ [39] for the complex [40, 41] as well as for NBO analysis. The X-ray structural data of complex **1** was used as input for the theoretical calculations. The structure of the ligand was extracted from the crystallographic information file of this complex and used for DFT studies.

References

[1] A. Kumari, *Sweet Biochemistry: Remembering Structures, Cycles, and Pathways by Mnemonics*, Academic Press, Amsterdam **2017**.

[2] K. S. Jain, T. S. Chitre, P. B. Miniyar, M. K. Kathiravan, V. S. Bendre, V. S. Veer, S. R. Shahane, C. J. Shishoo, *Curr. Sci.* **2006**, *90*, 793.

[3] K. R. A. Abdellatif, R. B. Bakr, *Bioorg. Chem.* **2018**, *78*, 341.

[4] C.-A. Lefebvre, E. Forcellini, S. Boutin, M.-F. Côté, R. C-Gaudreault, P. Mathieu, P. Lagüe, J.-F. Paquin, *Bioorg. Med. Chem. Lett.* **2017**, *27*, 299.

[5] A. Rahmouni, S. Souiei, M. A. Belkacem, A. Romdhane, J. Bouajila, H. Ben Jannet, *Bioorg. Chem.* **2016**, *66*, 160.

[6] C. Denneval, S. Achelle, C. Baudequin, F. Robin-le Guen, *Dyes Pigm.* **2014**, *110*, 49.

[7] E. V. Verbitskiy, E. M. Cheprakova, J. O. Subbotina, A. V. Schepochkin, P. A. Slepukhin, G. L. Rusinov, V. N. Charushin, O. N. Chupakhin, N. I. Makarova, A. V. Metelitsa, V. I. Minkin, *Dyes Pigm.* **2014**, *100*, 201.

[8] C. Tang, Q. Zhang, D. Li, J. Zhang, P. Shi, S. Li, J. Wu, Y. Tian, *Dyes Pigm.* **2013**, *99*, 20.

[9] E. V. Verbitskiy, A. A. Baranova, K. I. Lugovik, K. O. Khokhlov, E. M. Cheprakova, M. Z. Shafikov, G. L. Rusinov, O. N. Chupakhin, V. N. Charushin, *Dyes Pigm.* **2017**, *137*, 360.

[10] E. V. Verbitskiy, E. B. Gorbunov, A. A. Baranova, K. I. Lugovik, K. O. Khokhlov, E. M. Cheprakova, G. A. Kim, G. L. Rusinov, O. N. Chupakhin, V. N. Charushin, *Tetrahedron* **2016**, *72*, 4954.

[11] J.-W. Zhu, X.-C. Song, Y.-D. Lin, E. Yang, *Acta Crystallogr.* **2007**, *E63*, m1044.

[12] P. Arranz, C. Bazzicalupi, A. Bencini, A. Bianchi, S. Ciattini, P. Fornasari, C. Giorgi, B. Valtancoli, *Inorg. Chem.* **2001**, *40*, 6383.

[13] F. H. Allen, *Acta Crystallogr.* **2002**, *B58*, 380.

[14] M. A. Lemes, A. Pialat, S. N. Steinmann, I. Korobkov, C. Michel, M. Murugesu, *Polyhedron* **2016**, *108*, 163.

[15] Y.-H. Sun, S.-F. Luo, X.-Z. Zhang, Z.-Y. Du, *Acta Crystallogr.* **2009**, *E65*, m708.

[16] H.-M. Park, I.-H. Hwang, J.-M. Bae, Y.-D. Jo, C. Kim, H.-Y. Kim, Y.-M. Kim, S.-J. Kim, *Bull. Korean Chem. Soc.* **2012**, *33*, 1517.

[17] L. Saghatforoush, Z. Khoshtarkib, H. Keypour, M. Hakimi, *Polyhedron* **2016**, *119*, 160.

[18] B. Holló, Z. D. Tomić, P. Pogány, A. Kovács, V. M. Leovac, K. M. Szécsényi, *Polyhedron* **2009**, *28*, 3881.

[19] B. Hu, Q.-Q. Liu, T. Tao, K. Zhang, J. Geng, W. Huang, *Inorg. Chim. Acta* **2013**, *394*, 576.

[20] F. Marandi, K. Moeini, H. Krautscheid, *Acta Crystallogr.* **2019**, *C75*, 1389.

[21] Z. Mardani, V. Golsanamlou, S. Khodavandegar, K. Moeini, A. M. Z. Slawin, J. D. Woollins, *J. Coord. Chem.* **2018**, *71*, 120.

[22] Z. Mardani, V. Golsanamlou, S. Khodavandegar, K. Moeini, A. M. Z. Slawin, J. D. Woollins, *Z. Naturforsch.* **2017**, *72b*, 335.

[23] F. Marandi, K. Moeini, B. Mostafazadeh, H. Krautscheid, *Polyhedron* **2017**, *133*, 146.

[24] F. Marandi, K. Moeini, F. Alizadeh, Z. Mardani, C. K. Quah, W.-S. Loh, *Z. Naturforsch.* **2018**, *73b*, 369.

[25] L. Saghatforoush, K. Moeini, S. A. Hosseini-Yazdi, Z. Mardani, A. Hajabbas-Farshchi, H. T. Jameson, S. G. Telfer, J. D. Woollins, *RSC Adv.* **2018**, *8*, 35625.

[26] Z. Mardani, R. Kazemshoar-Duzduzani, K. Moeini, A. Hajabbas-Farshchi, C. Carpenter-Warren, A. M. Z. Slawin, J. D. Woollins, *RSC Adv.* **2018**, *8*, 28810.

[27] S. Shi, T. M. Yao, X. T. Geng, L. Chen, L. N. Ji, *Acta Crystallogr.* **2007**, *E64*, o272.

[28] CRYSALIS PRO Software System (version 1.171.38.41), Intelligent Data Collection and Processing Software for Small Molecule and Protein Crystallography, Rigaku Oxford Diffraction, Yarnton, Oxfordshire (UK) **2015**.

[29] G. Sheldrick, *Acta Crystallogr.* **2015**, *A71*, 3.

[30] G. Sheldrick, *Acta Crystallogr.* **2015**, *C71*, 3.

[31] O. V. Dolomanov, L. J. Bourhis, R. J. Gildea, J. A. K. Howard, H. Puschmann, *J. Appl. Crystallogr.* **2009**, *42*, 339.

[32] L. J. Farrugia, *J. Appl. Crystallogr.* **1997**, *30*, 565.

[33] M. N. Burnett, C. K. Johnson, ORTEP-III, Report ORNL-6895. Oak Ridge National Laboratory, Oak Ridge, TN, USA, **1996**.

[34] G. Bergerhof, M. Berndt, K. Brandenburg, *J. Res. Natl. Inst. Stand. Technol.* **1996**, *101*, 221.

[35] M. J. Frisch, G. W. Trucks, H. B. Schlegel, G. E. Scuseria, M. A. Robb, J. R. Cheeseman, G. Scalmani, V. Barone, B. Mennucci, G. A. Petersson, H. Nakatsuji, M. Caricato, X. Li, H. P. Hratchian, A. F. Izmaylov, J. Bloino, G. Zheng, J. L. Sonnenberg, M. Hada, M. Ehara, K. Toyota, R. Fukuda, J. Hasegawa, M. Ishida, T. Nakajima, Y. Honda, O. Kitao, H. Nakai, T. Vreven, J. A. Montgomery

Jr., J. E. Peralta, F. Ogliaro, M. J. Bearpark, J. Heyd, E. N. Brothers, K. N. Kudin, V. N. Staroverov, R. Kobayashi, J. Normand, K. Raghavachari, A. P. Rendell, J. C. Burant, S. S. Iyengar, J. Tomasi, M. Cossi, N. Rega, N. J. Millam, M. Klene, J. E. Knox, J. B. Cross, V. Bakken, C. Adamo, J. Jaramillo, R. Gomperts, R. E. Stratmann, O. Yazyev, A. J. Austin, R. Cammi, C. Pomelli, J. W. Ochterski, R. L. Martin, K. Morokuma, V. G. Zakrzewski, G. A. Voth, P. Salvador, J. J. Dannenberg, S. Dapprich, A. D. Daniels, Ö. Farkas, J. B. Foresman, J. V. Ortiz, J. Cioslowski, D. J. Fox, Gaussian 09., Gaussian, Inc., Wallingford, CT, USA, **2009**.

[36] J. P. Perdew, *Phys. Rev.* **1986**, *B33*, 8822.

[37] A. D. Becke, *J. Chem. Phys.* **1993**, *98*, 5648.

[38] R. Ditchfield, W. J. Hehre, J. A. Pople, *J. Chem. Phys.* **1971**, *54*, 724.

[39] P. J. Hay, W. R. Wadt, *J. Chem. Phys.* **1985**, *82*, 270.

[40] G. Abbas, A. Hassan, A. Irfan, M. Mir, R. Mariya Al, G. Wu, *J. Struct. Chem.* **2015**, *56*, 92.

[41] M. Ghiasi, S. Kamalinahad, M. Zahedi, *J. Struct. Chem.* **2014**, *55*, 1574.